



LUND UNIVERSITY

On performance of hidden car roof antennas

Yousaf, Irfan; Lau, Buon Kiong

Published in:

European Conference on Antennas and Propagation (EuCAP), 2018

2018

Document Version:

Peer reviewed version (aka post-print)

[Link to publication](#)

Citation for published version (APA):

Yousaf, I., & Lau, B. K. (2018). On performance of hidden car roof antennas. In *European Conference on Antennas and Propagation (EuCAP), 2018*

Total number of authors:

2

General rights

Unless other specific re-use rights are stated the following general rights apply:

Copyright and moral rights for the publications made accessible in the public portal are retained by the authors and/or other copyright owners and it is a condition of accessing publications that users recognise and abide by the legal requirements associated with these rights.

- Users may download and print one copy of any publication from the public portal for the purpose of private study or research.
- You may not further distribute the material or use it for any profit-making activity or commercial gain
- You may freely distribute the URL identifying the publication in the public portal

Read more about Creative commons licenses: <https://creativecommons.org/licenses/>

Take down policy

If you believe that this document breaches copyright please contact us providing details, and we will remove access to the work immediately and investigate your claim.

LUND UNIVERSITY

PO Box 117
221 00 Lund
+46 46-222 00 00

On Performance of Hidden Car Roof Antennas

Irfan Mehmood Yousaf^{1,2}, Buon Kiong Lau²

¹ Volvo Car Corporation, Gothenburg, Sweden, irfan.yousaf@volvocars.com

² Department of Electrical and Information Technology, Lund University, Lund, Sweden

Abstract—Hidden antenna solutions for car roofs are of current interest to car manufacturers, to avoid having larger shark-fin based antenna systems to support growing number of wireless services. However, there are only a few studies in the literature on the integration of hidden antennas, particularly in relation to realistic roofs and propagation channels. This paper investigates the performance impact of hiding car roof-top antennas in roof cavities for an outdoor channel defined by an angular power spectrum. Different 700 MHz antenna concepts and roof cavity locations are considered for an idealized flat roof as well as a real curved roof. The results reveal that hiding antennas in cavities result in a minor mean effective gain (MEG) penalty of up to 1 dB, for a flat rectangular car roof. However, a realistic roof curvature can largely offset the MEG loss. Moreover, different monopole-based antenna concepts can provide MEG variations of up to nearly 3 dB, indicating that significant performance gain can be achieved through an optimized design.

Index Terms—vehicular antenna, internal antenna, MEG.

I. INTRODUCTION

Similar to smartphones, the design of a car's appearance has become a key factor in determining the success of the car in the consumer market. In addition, potential customers are focusing more and more on the safety features and the connectivity functions offered by the car [1], [2]. Little attention is paid to the size and power of the engine, which used to be the key selling point. There is also a gradual shift towards autonomous drive, which puts higher demands on the car to be well aware of its surroundings as well as to be connected to the outside world via multiple wireless systems.

In recent years, antennas for wireless systems are usually placed on the rear part of the car roof. The size of these "shark fin" roof antennas has been increasing, due to an increasing number of wireless systems being supported [3]-[5]. This trend is in conflict with the growing interest to decrease the drag coefficient of hybrid and electric cars, to make the car battery last longer for an increased electric-driven range. Moreover, the current trend in replacing the plain car roof with a big panorama roof and even a complete glass roof also challenges the existence of a visible antenna system. In addition, from an aesthetic point of view, these shark fin antennas with their design constraints are becoming old-fashion and they do not match the styling of newer cars.

Therefore, there is a growing interest in developing hidden antenna solutions to replace the visible shark fin antennas [6]-[10]. Low *et al.* [6] studied the use of a cavity on the car roof for hidden antenna solutions. This concept

was proposed for antennas operating at AM (0.150-1.5 MHz), FM (88-108 MHz), DAB (217.5-230 MHz) and TV (470-862 MHz) frequencies. However, the study focused on the FM frequencies and did not consider the performance of the antennas for the higher frequencies. To improve safety and appearance of the roof antennas, efforts have also been made to lower the antenna height. For example, the low-profile LTE/GPS/satellite radio multiband antenna proposed in [7] has the height of 0.056 wavelength, at the lowest band of 830 MHz. Further studies have been done for narrowband [8], wideband [8], [9] and pattern reconfigurable [10] antennas within 0.7-6 GHz using the roof cavity concept.

Although comments are made in [6]-[10] on how well the radiation patterns of the proposed antennas meet some criteria in the upper hemisphere (e.g., high gain in the horizontal plane for good coverage), only paper [6] provides numerical and experimental evaluation with the channel (for FM antennas). Moreover, these antennas are mounted on a flat circular or square ground plane, e.g., $1 \times 1 \text{ m}^2$ [8], [10], which does not reflect realistic roof dimensions nor take into account the roof curvature inherent in the design of many modern cars. The curvature of the roof results in a specific inclination angle at the front and rear parts of the roof, which is typical 5° - 20° depending on the type of car. For example, the roofs of sports cars or sedan cars tend to have larger inclination angles in comparison to sports utility vehicles (SUVs) or station wagons.

In this context, this paper aims to provide useful insight into the effect of realistic roof curvature on the performance of several hidden antennas in a roof cavity, based on full-wave simulations. Different low-profile monopole-based hidden antennas and a quarterwave monopole covering LTE Band 13 (746-787 MHz) are utilized in order to examine the impact of antenna design. Moreover, the effect of the propagation channel is directly included in this simulation study by means of combining the antenna patterns with an outdoor channel defined by an angular power spectrum (APS).

II. SIMULATION SETUP

A. Reference Monopole and Monopole-based Antennas

In this paper, we focus on monopole and monopole-based antennas that offer monopolar (or monopole-like) antenna pattern. This is because monopolar antenna pattern is known to be desirable for terrestrial wireless communications (e.g., LTE), where the main directions of arrival (and departure) of radio signals tend to be

concentrated around the elevation angles of 60° - 90° (90° being the azimuth plane). In contrast, GPS antennas should provide good skyward coverage (e.g., small elevation angles), which makes patch antennas a suitable choice.

Four antennas are considered in this study. All the antennas are first mounted on a flat $1 \times 1 \text{ m}^2$ ground plane with no cavity and tuned to cover LTE Band 13 (746-787 MHz) at 6 dB impedance bandwidth (see Fig. 1). The antenna simulations were performed using the time-domain solver in the 2017 CST Microwave Studio software [11]. All the antennas and the ground planes are assumed to be perfect electric conductor (PEC).

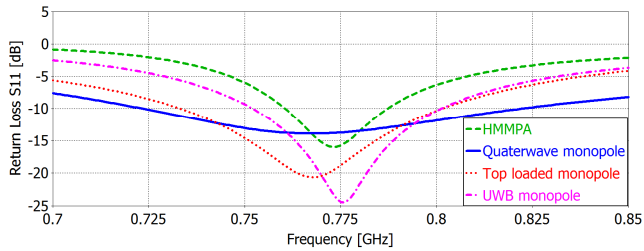


Fig. 1. Simulated reflection coefficients of four different antennas on a flat $1 \times 1 \text{ m}^2$ ground plane. The four antennas are shown in Fig. 2.

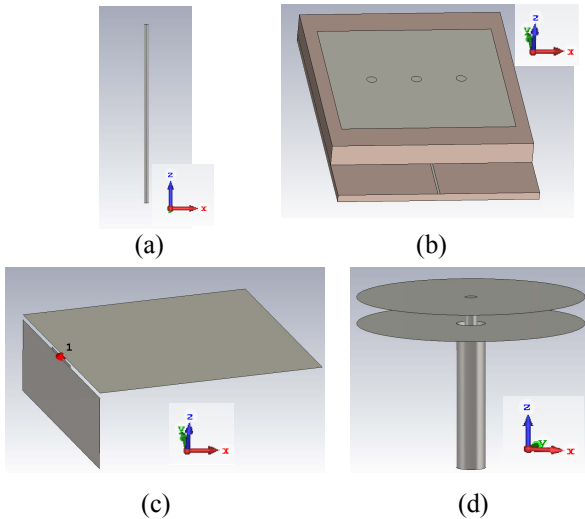


Fig. 2. 3D view of the simulated antennas: (a) $\lambda/4$ monopole, (b) HMMPA, (c) UWB antenna, (d) top-loaded monopole.

A quarterwave ($\lambda/4$) monopole antenna of height 94 mm, shown in Fig. 2(a), is used as a reference case. Even though it does not fit into the roof cavity considered in this paper, it provides a reference monopolar antenna pattern for the remaining three other antennas (see Figs 2(b)-2(d)) that were designed for low-profile but still maintaining monopolar operation (hence offering monopolar pattern). The second antenna, called Higher Mode Microstrip Patch Antenna (HMMPA) [12], is a low-profile antenna originally designed for on-body communications in body area networks (see Fig. 2(b)). It is designed to enhance radiation along the body surface, resulting in a monopolar pattern. Here, it is tuned to cover LTE Band 13 and the resulting outer dimensions are $90 \times 129 \times 13.5 \text{ mm}^3$. The third

antenna, called UWB antenna (see Fig. 2(c)), is a simplified version and of the low-profile wideband antenna in [9]. It was proposed for integration into a car roof cavity. It resembles a folded rectangular plate, with a 2 mm air gap along the folded edge. Around the center of the gap (for a length of 20 mm), the gap width is reduced to 1 mm. The antenna is fed using a discrete port (of length 1 mm) placed across the center of the air gap. The slit and the curved air gap in the original design in [9] were not incorporated. The dimensions of this antenna are $84 \times 84 \times 30 \text{ mm}^3$. The radiation pattern of this antenna is the least monopole-like antenna among the four antennas. This is because it does not have a null along the z -axis [9]. The final antenna (see Fig. 2(d)) is a top-loaded monopole, based on the design in [13]. The overall height is 32 mm and the gap between the top and bottom circular plates is 8 mm. The diameter of the circular plates is 35 mm.

B. Car Roof Models and Roof Cavity Model

Different car roof models were used in this study. Apart from the reference $1 \times 1 \text{ m}^2$ flat ground plane (no cavity). To examine the impact of having a larger ground plane, which better resembles the dimensions of a car roof (in this case, the car roof of Volvo S90), a flat ground plane of dimensions $1.667 \times 1.192 \text{ m}^2$ is used. The antenna was placed at the center, as for the $1 \times 1 \text{ m}^2$ case. To consider the impact of sinking the antennas into a roof cavity, two cavity locations were studied for the enlarged flat ground plane. The roof cavity considered in this paper is based on the cavity model in [8] and [10]. The depth of the cavity is 40 mm and the other dimensions are given in Fig. 3.

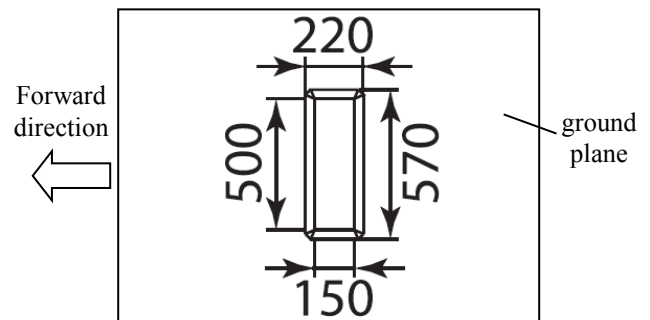


Fig. 3. Dimensions of roof cavity on a ground plane. The cavity depth is 40 mm. The forward direction of the car is indicated.

For the two cavity locations of the flat roof, one is in the center and another is in the rear part (i.e. identical to the front part, due to symmetry in this study), as shown in Figs. 4(a) and 4(b). The rear cavity is offset by 0.6 m from the center of the ground plane along the x axis.

To examine the impact of curvature on a real car roof, the car roof of Volvo S90 was chosen, for both cases of with and without sun roof (See Figs. 4(c) to 4(f)). For the case with no sun roof, three cavity locations (front, center and rear) were considered, as shown in Figs. 4(c) to 4(e). The front and rear positions are offset from the center of the curved roof by 0.462 m and 0.5 m, respectively, along the x axis. The inclination of the roof at the front and rear position

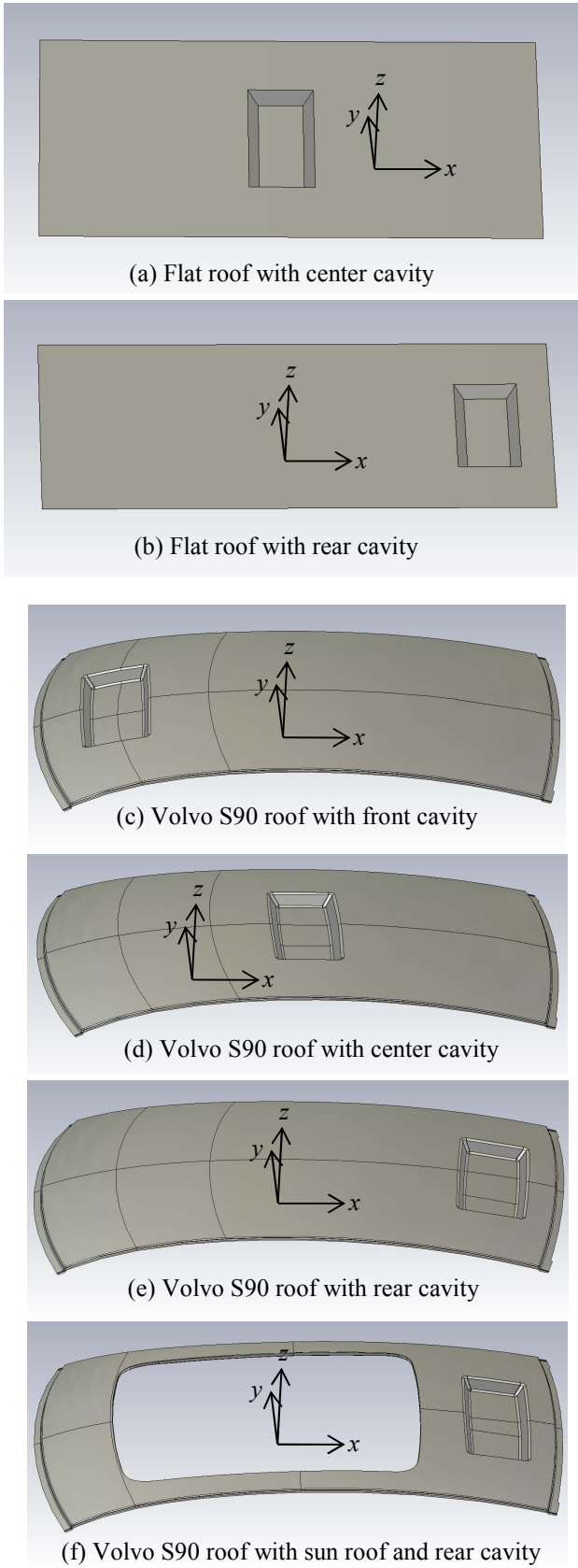


Fig. 4. 3D view of the simulated car roofs (flat, curved or curved with sun roof) with different cavity locations.

is approximately 10° . The impact of the sun roof on the performance is also investigated by using the car roof of Volvo S90 with the sun roof option, as shown in Fig. 4(f). In this case, only the rear cavity location can be considered.

C. Mean Effective Gain and Angular Power Spectrum

In a multipath environment, such as the vehicular channel considered in this paper, mean effective gain (MEG) can be used to evaluate the overall channel gain, given an APS and a 3D antenna pattern. MEG assumes channel gain averaging over a random route and it is defined as the ratio between the mean received power at a mobile antenna and the total mean incident power. In spherical coordinates, MEG can be calculated as [14]

$$MEG = \oint \frac{\gamma}{\gamma+1} G_\theta(\Omega) P_\theta(\Omega) + \frac{1}{\gamma+1} G_\phi(\Omega) P_\phi(\Omega) d\Omega, \quad (1)$$

where γ is the cross-polarization ratio (XPR), $\Omega = (\theta, \phi)$, $d\Omega = \sin\theta d\theta d\phi$, $G_\theta(\Omega)$ and $G_\phi(\Omega)$ are the θ and ϕ components of the antenna gain pattern, and $P_\theta(\Omega)$ and $P_\phi(\Omega)$ represent the θ and ϕ components of the incident APS. The antenna gain is the *realized* antenna gain, which includes mismatch, dielectric and conductive losses.

For an outdoor multipath environment, the APS can be modeled by a uniform distribution in the azimuth and a Gaussian distribution in the elevation, with the mean of $\theta = 80^\circ$ (or 10° from the azimuth plane) and the variance of 15° [15]. The APS is assumed to be identical for both polarizations and the XPR is given by $\gamma = 5$ dB. As a reference, the case of 3D uniform APS (i.e., uniform rich scattering from all directions) was evaluated. In this special case, $P_\theta(\Omega) = P_\phi(\Omega) = 1$ and $\gamma = 1$. The MEG for this case should be -3 dB, if the antenna is lossless and perfectly matched [16]. The MEG results were evaluated at the center frequency of 775 MHz, which means that the simulated 3D antenna patterns were extracted at this frequency.

III. RESULTS AND DISCUSSION

The simulated radiation patterns of the reference antenna (i.e., the $\lambda/4$ monopole) and the HMMPA in different cavity locations and roof models are shown in Figs. 5 and 6, respectively. To ease comparisons, the realized gain is shown for the range of -25 dB to 10 dB for all the pattern plots. The radiation patterns of these two antennas are shown as they are the extreme cases in terms of antenna height. The case of each of the antennas on the 1×1 m² ground plane (no cavity) is also added as a reference. In Fig. 5, it can be seen that there are only small variations in the $\phi = 90^\circ$ cut among different cavity locations for the $\lambda/4$ monopole. In contrast, there are more variations in the $\phi = 0^\circ$ (xz -plane) and $\theta = 90^\circ$ (azimuth plane) cuts due to the curvature of the roof along the x axis. Due to the flat surface in the middle of the curved car roof, the center cavity location gives a symmetric radiation pattern. For the HMMPA (see Fig. 6), the $\phi = 90^\circ$ cut seems to be more distorted (relative to monopolar pattern) in the curved roof cases except for the center cavity.

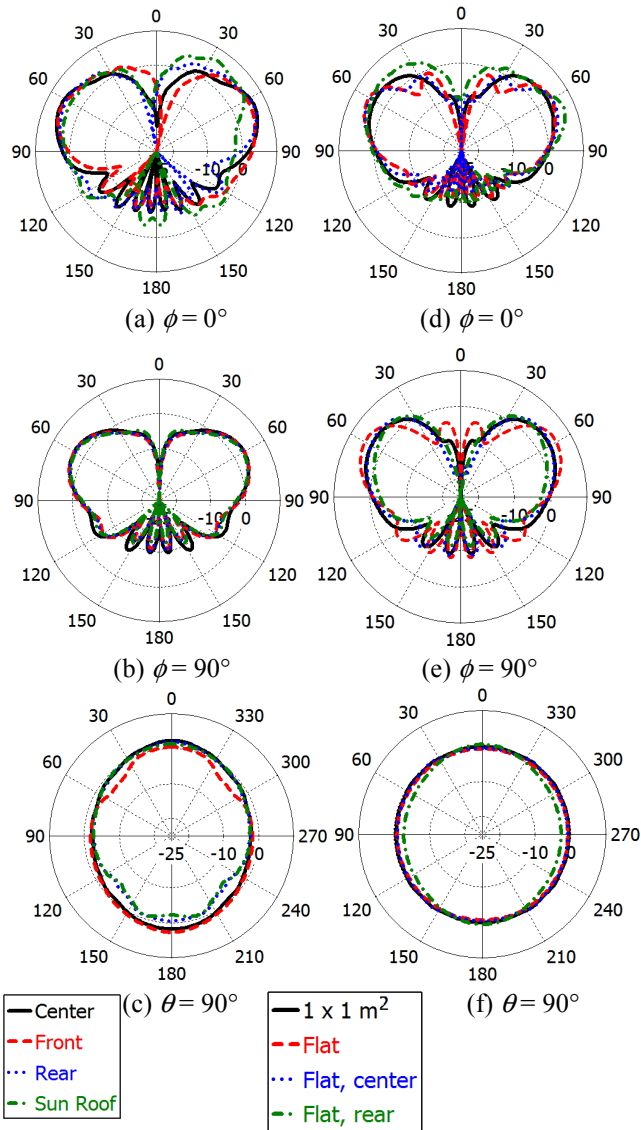


Fig. 5. 2D cuts of $\lambda/4$ monopole antenna patterns (realized gain) for the curved roof cases (all with cavity) in (a)-(c) and for the flat roof cases (without cavity or with cavity in center/rear) in (d)-(f).

TABLE I. SIMULATED MEG (dB) FOR OUTDOOR ENVIRONMENT

Roof Type	Cavity position	$\lambda/4$ Monopole	UWB antenna	HMMPA	Top loaded monopole
$1 \times 1 \text{ m}^2$	No cavity	0.35	-1.35	0	0.1
Flat roof	No cavity	0.82	-0.82	0.52	0.58
Flat roof	Center	0.41	-1.72	0.17	0.17
Flat roof	Rear	-0.093	-1.82	-0.37	-0.24
Curved roof	Front	0.34	-1.28	-0.14	0.13
	Center	0.77	-1.15	0.54	0.58
	Rear	0.09	-3	-0.34	-0.13
Curved with Sun Roof	Rear	-0.49	-2.7	-1.15	-0.71

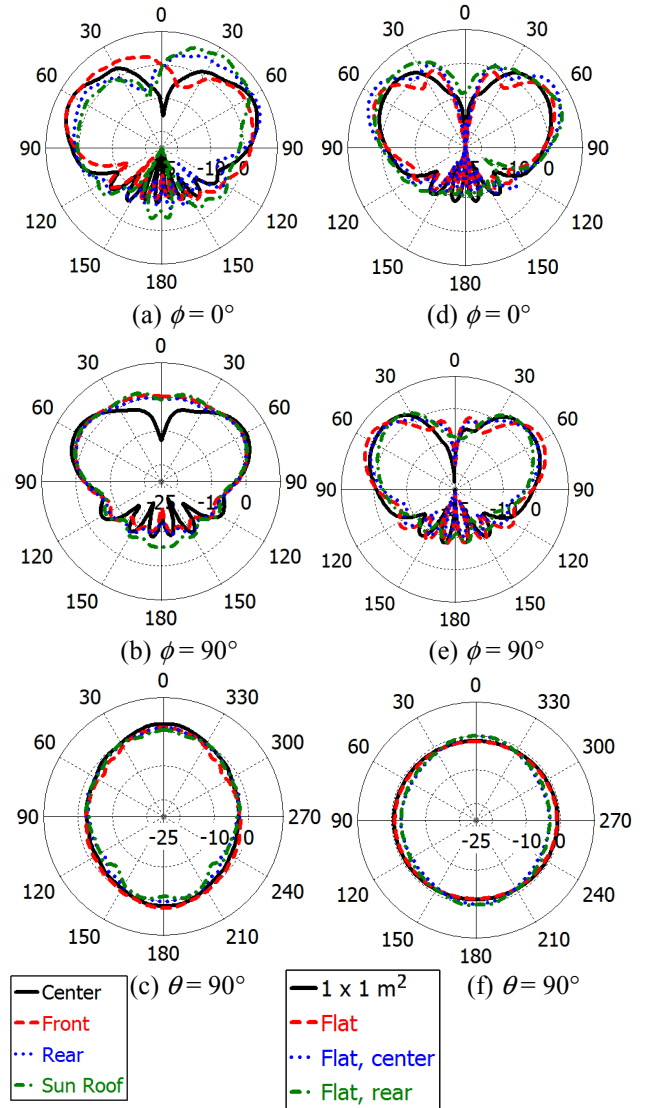


Fig. 6. 2D cuts of HMMPA patterns (realized gain) for the curved roof cases (all with cavity) in (a)-(c) and for the flat roof cases (without cavity or with cavity in center/rear) in (d)-(f).

The MEG for the 3D uniform APS is found to be around -3 dB for all cases, which is expected, since the antennas are lossless and well matched at the center frequency. Therefore, this reference MEG evaluation highlights the impact of the antenna pattern, the propagation channel and their mutual interaction on the achieved overall channel gain. For the outdoor (non-uniform) environment defined in Section II-C, the MEG results are summarized in Table I.

It can be seen that the flat ground plane with the size of the car roof has higher MEG compared to the $1 \times 1 \text{ m}^2$ ground plane. This can be attributed to the smaller ground plane causing the antenna pattern to tilt upwards [16], which may be observed for the $\lambda/4$ monopole and HMMPA in Figs. 5 and 6, respectively. A flat roof without any cavity is the optimal case for all antennas, as may be expected from the larger ground plane than the $1 \times 1 \text{ m}^2$ case and also having no obstruction from cavity walls. For the curved roof cases,

the highest MEG for all the antennas is achieved for the center cavity location, as any inclination of the roof results in some distortion in the symmetric monopolar pattern (i.e., pattern rotated by the inclination angle). Furthermore, it is also better than the flat roof center cavity case because the curved roof can provide less obstruction to the radiation along the azimuth plane.

For the flat roof with cavity in the center, the MEG around 0.5 dB better than the cavity in the rear, except for the UWB antenna. This is because the ground plane size around the cavity affects the monopolar patterns, but the UWB antenna is less affected due to its more significant upward radiation (i.e., like a patch but with less gain) [9]. There are some differences in the MEG for the front and the rear cavity locations for the curved roof due to a slight difference in inclination of the curved roof. The difference is larger for the UWB antenna case, due to more asymmetric pattern along the x axis. Another interesting comparison can be made for the curved roof, with and without sun roof. It can be seen that the sun roof case always has lower MEG due to the smaller size of the ground plane (especially in the vicinity of the cavity) [16].

Generally, we see that the different antennas show similar variations when compared among all the cases. The maximum variations in MEG for the $\lambda/4$ monopole, UWB antenna, HMMPA and top-loaded monopole are 1.3 dB, 2.18 dB, 1.69 dB and 1.29 dB, respectively. The UWB antenna has the worst performance since its radiation pattern is least monopolar (and patch-like in having significant upward radiation) [9], which implies poor matching to the defined outdoor channel with incident waves focused around the azimuth plane. For a curved roof, the center location of the cavity is the best and the rear location is the worst. Having a sun roof further degrades the MEG by approximately 0.5 dB. Finally, the design of the low-profile (hidden) antenna can result in significant differences in the MEG performance. In particular, the difference is nearly 3 dB between the UWB antenna and the top-loaded monopole for the curved roof with the rear cavity location. This highlights the need to design the hidden antenna for optimal performance, with the propagation channel being taken into account.

IV. CONCLUSION

This study focused on the performance of four antennas having monopole or monopole-like pattern, when each one is mounted in a roof cavity. The effect of roof curvature is also investigated. The results show that the antenna performance is best when the cavity is in the center of the roof when compared to the front and the rear locations. The sun roof case has the worst performance in comparison to other roof variants and cavity locations, due to pattern distortion from inclination (of rear cavity) and smaller ground plane. Possible future work includes the effect of the material of the cavity cover on antenna performance.

REFERENCES

- [1] R. Viereckl, J. Assmann, and C. Radüge, "In the fast lane – the bright future of connected cars," 2014. [Online]. Available: <https://www.strategyand.pwc.com/reports/in-the-fast-lane> [Accessed: Oct 20, 2017].
- [2] A. Meola, "Automotive industry trends: IoT connected smart cars and vehicles," 2016. [Online]. Available: <http://www.businessinsider.com/internet-of-things-connected-smart-cars-2016-10> [Accessed: Oct. 20, 2017]
- [3] N. Guan, H. Tayama, M. Ueyama, Y. Yoshijima, and H. Chiba, "A roof automobile module for LTE-MIMO antennas," in *Proc. IEEE-APS Topical Conf. Antennas Propag. Wireless Commun. (APWC' 2015)*, Turin, Italy, Sept. 7-11, 2015, pp. 387-391.
- [4] E. Ghafari, A. Fuchs, D. Eblenkamp, and D. N. Aloï, "A vehicular rooftop, shark-fin, multiband antenna for the GPS/LTE/cellular/DSRC systems," in *Proc. IEEE-APS Topical Conf. Antennas Propag. Wireless Commun. (APWC'2014)*, Palm Beach, FL, Aug. 3-9, 2014, pp. 237-240.
- [5] I. Goncharova and S. Lindenmeier, "A high efficient automotive roof-antenna concept for LTE, DAB-L, GNSS and SDARS with low mutual coupling," in *Proc. Europ. Conf. Antennas Propag. (EuCAP' 2015)*, Lisbon, Portugal, Apr. 13-17, 2015, pp. 1-5
- [6] L. Low, R. Langley, R. Breden, and P. Callaghan, "Hidden automotive antenna performance and simulation," *IEEE Trans. Antennas Propag.*, vol. 54, no. 12, pp. 3707-3712, Dec. 2006.
- [7] N. Guan, H. Chiba, Y. Yamaguchi, Y. Niihara, and H. Tayama, "A flat roof automobile antenna module for LTE, GPS and SDARS applications," in *Proc. IEEE-APS Topical Conf. Antennas Propag. Wireless Commun. (APWC'2014)*, Palm Beach, FL, Aug. 3-9, 2014, pp. 11-14.
- [8] G. Artner, R. Langwieser, and C. F. Mecklenbräuker, "Concealed CFRP vehicle chassis antenna cavity," *IEEE Antennas and Wireless Propag. Letters*, vol. 16, pp. 1415-1418, 2017.
- [9] N. Guan, H. Tayama, M. Ueyama, Y. Yamaguchi, and H. Chiba, "An invisible vehicle roof antenna," in *Proc. IEEE-APS Topical Conf. Antennas Propag. Wireless Commun. (APWC'2016)*, Cairns, Australia, Sep. 19-23, 2016, pp. 51-54
- [10] G. Artner, J. Kowalewski, C. F. Mecklenbräuker, and T. Zwick, "Pattern reconfigurable antenna with four directions hidden in the vehicle roof," in *Proc. Int. Workshop Antenna Technol. (iWAT' 2017)*, Athens, Greece, Mar. 1-3, 2017, pp. 82-85.
- [11] <https://www.cst.com/products/cstmws>
- [12] G. A. Conway and W. G. Scanlon, "Antennas for over-body-surface communication at 2.45 GHz," *IEEE Trans. Antennas Propag.*, vol. 57, no. 4, pp. 844-855, Apr. 2009.
- [13] L. Akhoondzadeh-Asl, J. Hill, J.-J. Laurin, and M. Riel, "Novel low profile wideband monopole antenna for avionics applications," *IEEE Trans. Antennas Propag.*, vol. 61, no. 11, pp. 5766-5770, Nov. 2013.
- [14] T. Taga, "Analysis for mean effective gain of mobile antennas in land mobile radio environments," *IEEE Trans. Veh. Technol.*, vol. VT-39, no. 2, pp. 117-131, May 1990.
- [15] Z. Ying and V. Plicanic, "Characterization of multi-channel antenna performance for mobile terminal by using near field and far field parameters," in *COST 273, TD(04) 095*, Goteborg, Sweden, Jun. 2004.
- [16] R. Vaughan and J. Bach Andersen, *Channels, Propagation and Antennas for Mobile Communications*. London: IEE, 2003, Ch. 8.